Magnetization-graded multiferroic composite and magnetoelectric effects at zero bias

S. K. Mandal,[1] G. Sreenivasulu,[1] V. M. Petrov,[1,2] and G. Srinivasan[1]

[1]*Physics Department, Oakland University, Rochester, Michigan 48309, USA*

[2]*Institute of Electronic and Information Systems, Novgorod State University B. S. Peterburgskaya St. 41, 173003 Veliky Novgorod, Russia*

(Received 16 November 2010; revised manuscript received 23 March 2011; published 29 July 2011)

A magnetoelectric (ME) phenomenon in a multiferroic composite consisting of magnetization-graded ferromagnetic and ferroelectric phases is discussed. The traditional strain mediated coupling in such composites arises due to magnetostriction and piezoelectric effects associated with the ferroic phases. Such an ME effect, in general, requires a bias magnetic field H_0 and an ac magnetic field. This paper is on the observation and theory of ME interactions under zero bias ($H_0 = 0$) in a bilayer of lead zirconate titanate (PZT) and a ferromagnetic layer in which the magnetization is graded with the use of Ni and Metglas. At low frequencies, the ME coefficient ranges from 0.3 to 1.6 V/cm Oe and depends on the thickness of the Metglas. A similar dependence is also observed for the ME coupling at bending modes. A factor of 40 increase in the ME voltage is measured at resonance. The zero-bias ME coupling is attributed to strain-mediated coupling between the transverse magnetization due to magnetization grading at the interface of Ni-Metglas and the in-plane ac magnetic field. Theoretical estimates of ME coefficients at low frequencies and bending modes are in general agreement with the data.

DOI: 10.1103/PhysRevB.84.014432 PACS number(s): 75.80.+q, 77.65.Fs, 75.50.Bb

I. INTRODUCTION

Single-phase multiferroics and composites of ferromagnetic and ferroelectric phases have attracted considerable interest in recent years due to a rich variety of phenomena associated with cross coupling between ferroic subsystems and strain mediated magnetoelectric (ME) interactions in composites.[1–10] The strain-mediated coupling in composites, in general, is observed as an induced electric field δE under an applied bias magnetic field H_0 and an ac field δH. The ME voltage coefficient $\alpha_E = \delta \mathrm{E}/\delta \mathrm{H}$ is measured as a function of H_0 and the frequency f of the ac field.[6–10] Studies on samples with ferromagnetic metals or alloys, ferrites, or manganites for the magnetic phase and lead zirconate titanate (PZT) or lead magnesium niobate–lead titanate (PMN-PT) for the piezoelectric phase reveal a giant low-frequency coupling and enhancement of the coupling strength when the electric or magnetic subsystem is at resonance.[6–12]

This paper is on ME interactions in a ferroic composite in which the order parameter is graded. Recent works on functionally graded ferroics have resulted in the discovery of important phenomena including internal potentials, induced anisotropies, and spontaneous strain.[13–15] Since the piezoelectric (d) and piezomagnetic (q) coefficients are the critical parameters that determine the strength of ME coupling in a composite, we recently modeled the effects of such grading in bilayers of Ni-Zn ferrite and PZT. Grading of magnetostriction λ (and $q = \delta\lambda/dH$) in the ferrite and piezoelectric coupling d was considered. A bilayer in which q and d are graded along a vertical axis, for example, will result in a bending moment that will have in-plane components that will affect the strength of ME interactions. Our theory predicts a 50%–60% stronger ME interaction in q and d graded ferrite-ferroelectrics compared with homogeneous systems.[16,17] Results of experiments on such graded systems are in agreement with the theory.[18]

This paper is on the observation and theory of ME effects in magnetization-graded ferromagnetic-piezoelectric layered composites. Ban *et al.* reviewed experiments and theoretical modeling on graded ferroics with particular emphasis on polarization (P) graded ferroelectrics.[19] In a film in which P is graded along an axis perpendicular to the sample plane, the grading in P manifests as a vertical shift in the P vs. E loop when excited with a periodic ac field in a modified Sower-Tower circuit. Significant modeling efforts in this regard include domain structures in graded ferroelectric films and multilayers.[20,21] Similar studies on magnetization-graded ferromagnets reveal the presence of an internal field.[22,23] In samples of composition-graded Ni-Zn ferrite, ferromagnetic resonance data indicated a "built-in" magnetic field aligned along the magnetization-gradient.[22] Similarly in a hexagonal ferrite with a variation in saturation magnetization of 30 emu/g over a sample thickness of 2.5 mm, the dc magnetization showed an anisotropy depending on the direction of the external magnetic field relative to the grading direction. A shift in magnetic properties corresponding to an internal magnetic field of 30 Oe was reported.[23] Such internals fields, in turn, give rise to zero-bias ME coupling in multiferroic composites.[18,24]

Here we focus on ME effects in a bilayer of PZT and a magnetization-graded ferromagnetic layer consisting of Ni (with $4\pi \mathrm{M} \approx 6$ kG) and Metglas ($4\pi \mathrm{M} \approx 15.6$ kG). Studies were performed on samples of PZT-Ni-Metglas and PZT-Metglas-Ni. Measurements of ME voltage coefficients (MEVCs) α_E vs. bias field H_0 at low frequencies and α_E vs. f at bending resonance show characteristics typical of piezomagnetic-piezoelectric cross coupling. The most significant observation, however, is the observation of ME coupling at zero bias ($H_0 = 0$). We attribute the coupling to the interaction of an out-of-plane internal magnetic field arising from grading in M and the applied in-plane ac magnetic field. Results of a systematic study on the dependence of the low frequency and resonance zero-field MEVC $\alpha_{E,0}$ on the thickness of ferromagnetic layer are provided here. A theory is also discussed for the effect and compared with data.

II. EXPERIMENT

Samples of Ni-Metglas-PZT and Metglas-Ni-PZT were studied. Annealed, 99.98% pure Ni foil (obtained from Goodfellow Cambridge Limited, England) of thickness 250 μm was used. The foil was polished down to a thickness

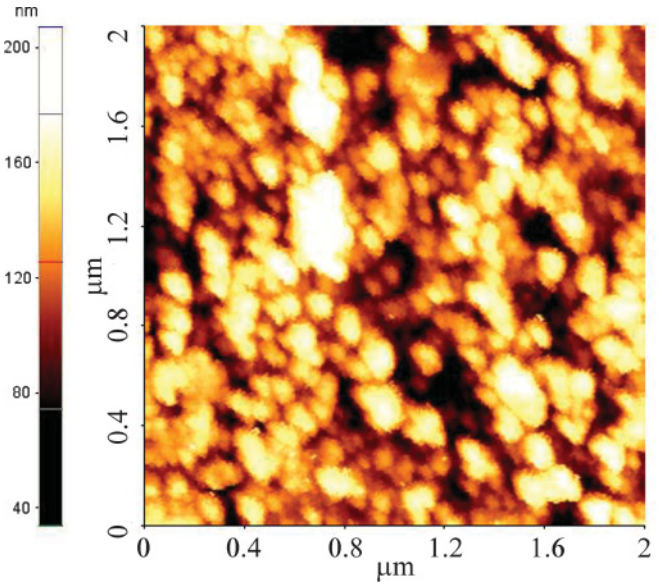

FIG. 1. (Color online) AFM topography for nickel showing 150–200-nm grains.

of 160 μm. Surface profile data obtained with a Park Systems scanning probe microscope (XE-100E) for the Ni foil is shown in Fig. 1. The thick film was polycrystalline with a grain size in the range 150–200 nm. We used iron-based Metglas (No. 2605SA-1 provided by Metglas Inc., Conway, SC) ribbons. The ribbons were 25 μm in thickness and contained 20–50nm crystallites, as seen in the atomic force microscopy (AFM) topography data in Fig. 2. Vendor-supplied PZT (No. 851, American Piezo Ceramics, Mackeyville, PA) was used in the composites.

Samples were made with 5 cm × 1 cm × 0.025 cm PZT, 160-μm-thick Ni, and 25-μm-thick Metglas of similar lateral dimensions. The PZT with silver electrodes was initially poled in an electric field of 30 kV/cm by heating it to 150 °C

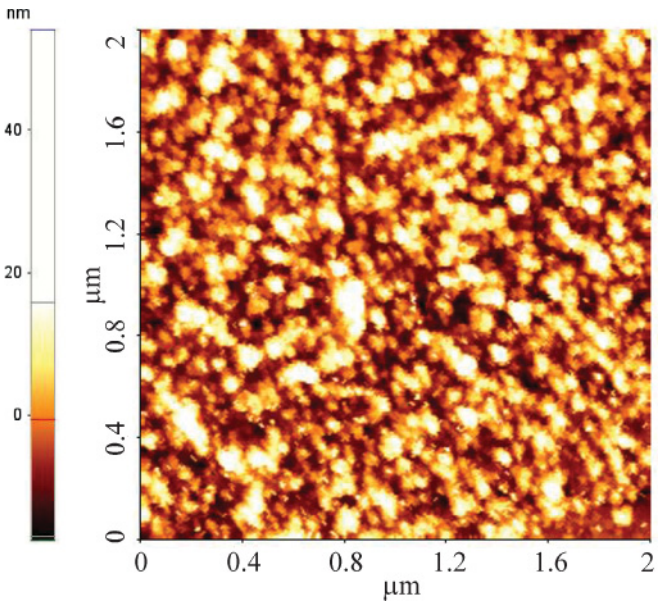

FIG. 2. (Color online) AFM topography for Metglas showing 20–50-nm crystallites.

in an oil bath. It was then bonded to Ni and Metglas with a 2- to 3-μm-thick layer of epoxy (West System 105-resin and 206-hardner). The sample was kept at 40 °C for 5 h to cure the epoxy. For samples with higher thicknesses of Metglas, it was necessary to bond the required number of 25-μm-thick Metglas layers with the epoxy. For ME characterization, a three-teriminal sample holder was used. Measurements were then made by subjecting the sample to a bias magnetic field H_0 generated by an electromagnet and ac magnetic field $H_1 =$ 1 Oe produced by a pair of Helmholtz coils. With the sample plane defined as (1,2), the magnetic fields were applied parallel to the length of the sample plane, along direction 1. The induced ac electric field E_3 was measured across the width of PZT, perpendicular to the bilayer plane. The MEVC $\alpha_E = E_3/H_1 = \delta V/t\delta H$, where t is the total thickness of PZT, was measured as a function of H_0 and frequency f of the ac magnetic field.

For measurements of ME voltages under zero-bias condition, a three-layer mu-metal magnetic shield was used to screen the effects of the Earth's magnetic field. The sample was subjected to ac fields $H_1 =$ 100–900 μOe and the voltage across the sample was amplified with a low-noise high-input impedance amplifier (Stanford Research Systems, Model SR560) and fed to a spectrum analyzer (Stanford Research Systems, Model SR780).

III. RESULTS

Representative data on variations of the MEVC α_E with H_0 are shown in Fig. 3 for PZT-Ni-Metglas and PZT-Metglas-Ni

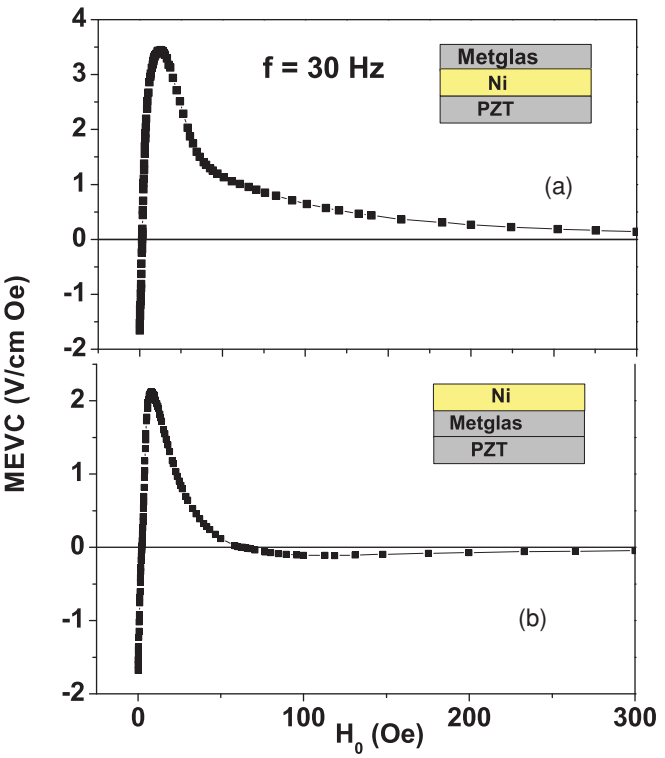

FIG. 3. (Color online) Magnetoelectric Voltage (MEVC) as a function of the bias field H_0 for samples of PZT and ferromagnetic layers with Ni and Metglas. The Metglas thickness is 75 μm. The bias field H_0 and ac field H_1 are parallel to the sample plane.

samples. The data are for a Metglas thickness of 75 μm. Consider first the data for PZT-Ni-Metglas in Fig. 3(a). The MEVC is ~1.6 V/cm Oe for $H_0 = 0$. There is a phase difference $\phi = 180^o$ between the applied ac magnetic field H_1 and the induced ME voltage δV. With increasing H_0 the magnitude of the MEVC decreases to zero for a bias field of 5–7 Oe. Beyond this zero crossing, a further a increase in the bias field results in a sharp increase in the MEVC to a maximum value of 3.5 V/cm Oe. Finally one observes a drop in the MEVC down to zero with increasing bias field. Data in Fig. 3(b) for PZT-Metglas-Ni shows similar MEVC vs. H_0 characteristics, but the peak MEVC is somewhat smaller than the value in Fig. 3(a).

An observation of significance in Fig. 3 is the large α_E for $H_0 = 0$. The large zero-bias MEVC can only be due to a torque which arises from interaction between the in-plane ac field H_1 and a transverse grading-induced magnetization. Compositional grading of ferrites are shown to result in such an internal field.[22,23] The torque produces a bending moment in the magnetic-layer direction and gives rise to the ME output at the zero-magnetic-bias field. An increase in in-plane bias field H_0 causes a gradual shift of effective magnetization toward the sample plane. As a result, the torque vanishes when the net magnetization is parallel to H_1.

The MEVC data beyond the zero crossing originate from strain-mediated coupling that arises due to piezomagnetism associated with the magnetic layer and the piezoelectric coupling for PZT. This effect is not considered any further in this paper.

Next we investigated the zero-field ME effects in detail. The PZT-Ni-Metglas sample was located in a magnetically shielded chamber to achieve $H_0 = 0$ and subjected to an in-plane ac field of 100 μOe. The ME voltage was measured with a spectrum analyzer. Results of these measurements are shown in Fig. 4. One observes a near-constant ME response independent of the frequency f of the ac field. The MEVC corresponds to 0.5 V/cm Oe and is smaller than the value in Fig. 3.

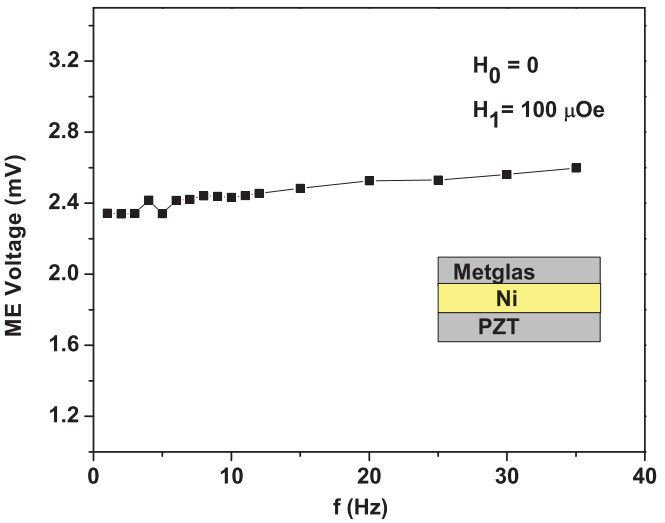

FIG. 4. (Color online) The zero-bias ME voltage as a function of frequency f of the ac field H_1 measured for a sample of PZT-Ni and 75-μm-thick Metglas.

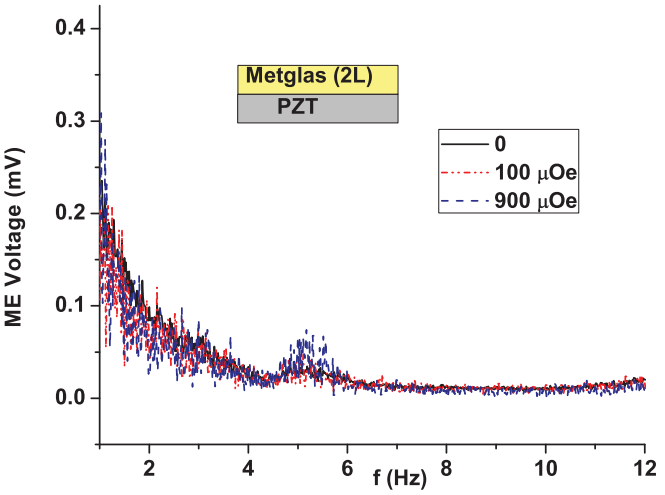

FIG. 5. (Color online) Data on ME voltage vs. frequency for a sample of PZT-50 μm Metglas. The profiles are for ac field $H_1 = 0$, 100 μOe, and 900 μOe at 1 Hz.

To confirm the absence of zero-field ME voltage in homogeneous bilayers, measurements similar to those in Fig. 4 were performed on PZT-Metglas or PZT-Ni. Representative data are shown in Fig. 5 for PZT and 50-μm-thick Metglas. The figure shows the ME voltage measured with a spectrum analyzer for ac fields of zero, 100 μOe, and 900 μOe. It is clear from the data that the ME voltage does not increase above the noise level even for $H_1 = 900$ μOe.

Next we focus on the zero-bias ME coupling in magnetization-graded samples. We prepared samples with Metglas thicknesses varying from 25 to 125 μm (or the number of layers $L = 1$–5) and measured the ME response as in Fig. 3. Figure 6 shows $\alpha_{E,0}$ as a function of L for the magnetization-graded samples. With increasing Metglas thickness, one observes a rapid rise in $\alpha_{E,0}$ to a peak value for $L = 3$ that is followed by a sharp fall for higher L. The zero-bias ME voltage is vanishingly small for $L = 5$.

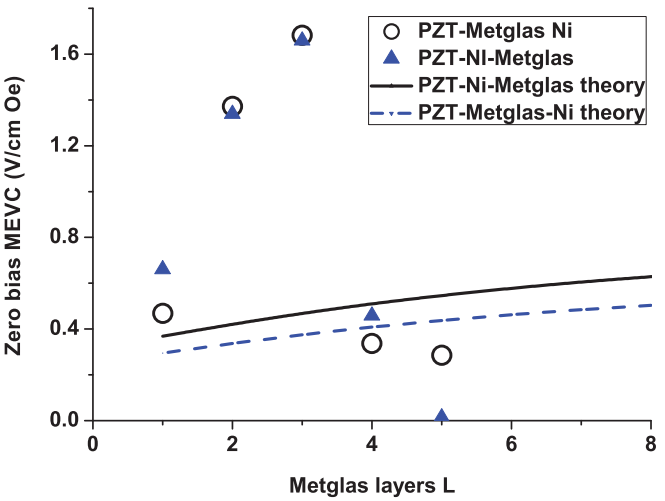

FIG. 6. (Color online) Zero-bias MEVC obtained from data as in Fig. 3 as a function of number of Metglas layers L for magnetization graded samples. The lines represent theoretical values.

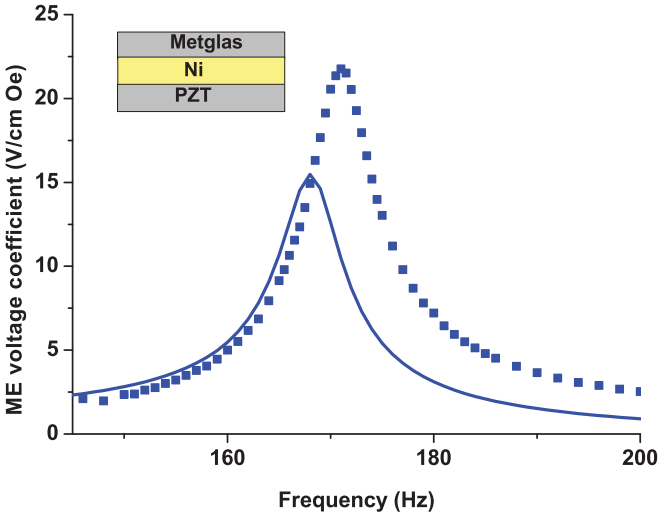

FIG. 7. (Color online) Magnetoelectric Voltage Coefficient for $H_0 = 0$ as a function of frequency f of the ac magnetic field H_1 for a sample of PZT-Ni-25 μm thick Metglas. The peak in the MEVC corresponds to bending resonance in the sample clamped at one end. The symbols are data and the solid line is theoretical estimates.

An ME phenomenon of interest is the coupling at bending resonance.[25–28] We modeled the resonance enhancement of ME interactions at frequencies corresponding to bending oscillations. It was shown that the enhancement in ME coupling occurs at the lowest frequency for a bilayer that is fixed at one end and free at the other end. Measurements of the zero-bias MEVC as a function of frequency of the ac magnetic field were carried out in the magnetically shielded chamber, and typical results are shown in Fig. 7. The data are for a sample of PZT-Ni-25-μm-thick Metglas. With increasing f, one notices an increase in $\alpha_{E,0}$ to a peak value at the resonance frequency of 170 Hz and a decrease to an off-resonance value at 200 Hz. The resonance value of the MEVC is a factor of 40 higher that the low-frequency value.

Similar measurements on samples with a series of Metglas thickness and the peak $\alpha_{E,0}$ are shown in Fig. 8. The data reveal a much stronger ME coupling at resonance in PZT-Ni-Metglas

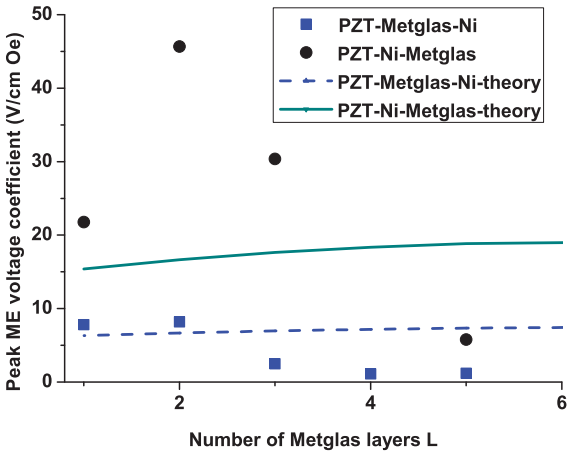

FIG. 8. (Color online) The resonance value of zero-bias MEVC vs. number of Metglas layers in the magnetization-graded samples. The solid and dashed lines are theoretical values.

than for PZT-Metglas-Ni. The peak value of $\alpha_{E,0}$ ranges from 2 to 46 V/cm Oe, depending on the thickness of the Metglas. The highest value is measured for PZT-Ni-75-μm Metglas.

Finally we compare the strength of zero-bias ME effects in the present system with observations in PZT-Ni-Zn ferrite[18] and laminates with a layer of metallic nickel and a layer of Ni-Zn ferrite particles dispersed in a lead-free piezoelectric.[19] The zero-field MEVCS, in Refs. 18 and 19 range from 25 to 100 mV/cm Oe, depending on the volume fraction for the piezoelectric and magnetic phases. The highest MEVC measured in the present paper is a factor of 16 higher than in PZT and composition-graded Ni-Zn ferrite.[18]

IV. THEORY

We discuss here a model for the zero-bias ME effects for PZT, Ni, and Metglas, as in Fig. 3. Although magnetic metals or alloys of homogeneous compositions are not piezomagnetic, one can achieve a pseudo-piezomagnetic effect ($q = d\lambda/dH$, where λ is the magnetostriction) by subjecting the sample to a bias magnetic field H_0 and ac field H_1. Magnetostriction of magnetic components and piezoelectric coupling of PZT are known to result in the traditional strain-mediated ME effect. However, there is a distinctive feature of a magnetic layer with graded saturation magnetization: Magnetically graded ferromagnets are shown to develop a built-in magnetization.[22,23] This magnetization gives rise to a new type of ME coupling that is a product property of spontaneous magnetization and piezoelectric coupling. The physical mechanism for this ME effect is as follows: The built-in magnetization interacts with applied ac magnetic field and thus produces a moment of rotation acting on the magnetic layers. Considering the sample as a cantilever, a flexural deformation arises which is transferred to the PZT layer. An induced output voltage is generated by average longitudinal stress in the piezoelectric phase. It should be noted that magnetic layers do not have to be magnetostrictive to exhibit such magnetoelectric coupling.

We assume a sample geometry and field orientations as in Fig. 9. The analysis described here is based on the well-known equations for the strain of magnetostrictive and piezoelectric phases and electric displacement of the latter:

$$\begin{aligned} {}^{m1}S_i &= {}^{m1}s_{ij}{}^{m1}T_j, \\ {}^{m2}S_i &= {}^{m2}s_{ij}{}^{m2}T_j, \\ {}^{p}S_i &= {}^{p}s_{ij}{}^{p}T_j + {}^{p}d_{ki}{}^{p}E_k, \\ {}^{p}D_k &= {}^{p}d_{ki}{}^{p}T_i + {}^{p}\varepsilon_{kn}{}^{p}E_n, \end{aligned} \tag{1}$$

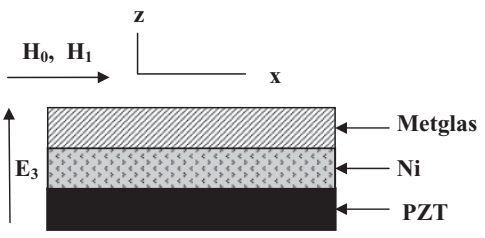

FIG. 9. A sample of PZT, Ni, and Metglas. The bias magnetic field H_0 and the ac magnetic field H_1 are parallel to the x axis. The piezoelectric layer is poled along z and the ac electric field E_3 is measured across PZT.

where S_i and T_j are strain and stress tensor components, E_k and D_k are the vector components of electric field and electric displacement, s_{ij} and d_{ki} are compliance and piezoelectric coefficients, and ε_{kn} is the permittivity matrix. The superscripts p, m_1 and m_2 correspond to piezoelectric and two magnetic layers, respectively. We assume the symmetry of piezoelectric to be ∞m and the magnetic layers to be cubic.

A. Low-frequency magnetoelectric effect

For finding the low-frequency MEVC at a no-bias magnetic field, we solve elastostatic and electrostatic equations in the piezoelectric phase and elastostatic equations in magnetic layers in the absence of magnetostrictive coupling. The modeling of ME coupling in bilayers based on a compositionally graded magnetostrictive component is described in our previous work.[17] In our actual investigation, we proceed from the theoretical approach cited above. To adapt that model to the structure in Fig. 9, we set the piezomagnetic coupling coefficients equal to zero. Next we assume the longitudinal axial strains of each layer to be linear functions of the vertical coordinate z_i to take into account the cylindrical bending of the trilayer: ${}^{p}\mathrm{S}_1 = {}^{p}S_{10} + z_p/\mathrm{R}_1$ ${}^{m1}S_1 = {}^{m1}S_{10} + \mathrm{z}_{m1}/R_1$, and ${}^{m2}S_1 = {}^{m2}S_{10} + \mathrm{z}_{m2}/R_1$, where ${}^{i}S_{10}$ are the centroidal strains along the $x$axis at $z_i = 0, R_1$ is the radius of curvature, and z_i is measured relative to centroidal plane of the i layer. It can be shown that centroidal strains obey the following conditions: ${}^{m2}S_{10} - {}^{m1}S_{10} = h_2/R_1$ and ${}^{m1}S_{10} - {}^{p}S_{10} = h_1/R_1$, where $h_1 = ({}^{m1}t + {}^{p}t)/2$ and $h_2 = ({}^{m1}\mathrm{t} + {}^{m2}\mathrm{t})/2$ are distances between the centroidal planes of the piezoelectric and first magnetic layers and between that of two magnetic layers, and ${}^{p}t$, ${}^{m2}t$, and ${}^{m2}t$ are thicknesses of three layers.

The axial forces in the three layers must add up to zero, and the rotating moments of axial forces in the three layers must be counteracted by resultant bending moments ${}^{p}J_2$, ${}^{m1}J_2$, and ${}^{m2}J_2$, induced in piezoelectric and two piezomagnetic layers to preserve force and moment equilibrium:

$$\begin{aligned} {}^{m1}F_1 + {}^{m2}F_1 + {}^{p}F_1 &= 0, \\ {}^{m1}F_1 h_1 + {}^{m2}F_1(h_1 + h_2) &= {}^{p}J_2 + {}^{m1}J_2 + {}^{m2}J_2 + {}^{H}J_2, \end{aligned} \tag{2}$$

where ${}^{i}F_1 = \int_{-{}^{i}t/2}^{{}^{i}t/2} {}^{i}T_1 dz_1$, ${}^{i}J_2 = \int_{-{}^{i}t/2}^{{}^{i}t/2} z_i^i T_1 dz_i$ and ${}^{H}J_2$ is a moment of rotation produced by the applied ac magnetic field. This rotating moment per unit width due to built-in magnetization is defined as

$${}^{H}J_2 = \mu_0 H_1({}^{1}M^{m1}t + {}^{2}M^{m2}t), \tag{3}$$

where ${}^{1}M$ and ${}^{2}M$ are vertical components of built-in magnetizations of magnetic layers arising from the stepped-graded magnetic phase.

The built-in magnetization due to grading in saturation magnetization can be estimated using the thermodynamic analysis similar to the polarization of a ferroelectric bilayer with different values of saturation polarization.[20,21] We consider a bilayer of two magnetic layers with normally directed magnetizations of layers. The free energy density of the bilayer can be presented as follows:

$$\begin{aligned} F = {} & v_1 \left[F_1({}^{1}m) - \mu_0 {}^{1}M H + \mu_0 \frac{N_{33}{}^{1}M^2}{2} \right] \\ & + v_2 \left[F_2({}^{2}m) - \mu_0 {}^{2}M H + \mu_0 \frac{N_{33}{}^{2}M^2}{2} \right] \\ & + \mu_0 v_1 v_2 \frac{({}^{1}M - {}^{2}M)^2}{2}, \end{aligned} \tag{4}$$

where $v_1 = t_1/(t_1+t_2), v_2 = t_2/(t_1+t_2)$, ${}^{1}M$ and ${}^{2}M$ are the volume fractions and the macroscopical magnetizations of layers, respectively, M is an average magnetization, $F_i({}^{i}m)$ is the free-energy density of the i layer as a function of the microscopic magnetization ${}^{i}m$, and H is the external magnetic field. For the polydomain layer, ${}^{i}M$ is dependent on fractions of 180° domains, β_i, and ${}^{i}M = (1–2\,\beta_i)^{i}m$. It is well known that domains prefer to be parallel or antiparallel to the easy magnetization axis, if any. In our case, the internal magnetic field due to mismatch in saturation magnetizations is high enough and is similar to an easy magnetization axis for the layer with lower saturation magnetization. Thus a majority of first-layer domains are parallel to the z axis. For the second layer (with higher saturation magnetization), the in-plane average magnetization components are zero at the zero-bias field provided that the easy-axis anisotropy field direction is parallel to the z axis. Thus the only z component of the second layer's average magnetization is nonzero due to the axial symmetry of the structure. The term $\mu_0 \frac{N_{33}{}^{i}M^2}{2}$ in Eq. (4) is the demagnetization energy and N_{33} is the form factor of the sample.

The last term in Eq. (4) expresses the magnetic coupling between the layers which arises due to the mismatch of the equilibrium magnetization of layers. Free-energy density is known to include only even powers of magnetization. An additive term which describes mismatch in a layer's magnetization should be zero for equal magnetizations. Thus the dominant term in free-energy expansion can be $k({}^{2}M–{}^{1}M)^2$. Then this term should be zero for each of the two layers separately. So we can put $k = \mu_0 v_1 v_2/2$. Ni and Metglas have a high value of $({}^{2}M - {}^{1}M)$ and all the discussion above and the form of Eq. (4) correspond to this system.

The free-energy density of the i layer can be determined by a Landau expansion as follows

$$F_i({}^{i}m) = \frac{a_i}{2}{}^{i}m^2 + \frac{b_i}{2}{}^{i}m^4, \tag{5}$$

where a_i and b_i are the Landau-type bulk free-energy expansion coefficients. For uncoupled layers, ${}^{1}m = {}^{1}M_0$ and ${}^{2}m = {}^{2}M_0$ where ${}^{1}M_0$ and ${}^{2}M_0$ are the saturation magnetizations of the layers. We assume next that ${}^{1}M_0 < {}^{2}M_0$.

The magnetizations in the coupled layers are determined by equations of equilibrium, $\partial F/\partial {}^{1}M = 0$ and $\partial F/\partial {}^{2}M = 0$. Taking into account Eq. (5) for F_1 and F_2, these equations are reduced to the form

$$\begin{aligned} \frac{\partial F_1}{\mu_0 \partial({}^{1}M)} &= H - N_{33}{}^{1}M + v_2({}^{2}M - {}^{1}M), \\ \frac{\partial F_2}{\mu_0 \partial({}^{2}M)} &= H - N_{33}{}^{2}M - v_1({}^{2}M - {}^{1}M). \end{aligned} \tag{6}$$

In the absence of an external field, these equations have an infinite number of solutions including the domain structure

with zero net magnetization ($\beta_1 = \beta_2 = 1/2$). In light of Eqs. (6), the mismatch in magnetizations of layers results in an additional magnetic field in the layer with lower magnetization (layer 1), which gives rise to an increase in magnetization. On the other hands, the additional field in the second layer is negative and appears a depolarizing field. Equations (6) can be reduced to an algebraic system of equations that is solved for ${}^1M$ and ${}^2M$ at fixed values of β_1 and β_2. The final solutions should result in minimum energy. For the bilayer of Ni and Metglas with $t_1 = 0.16$ mm and $t_2 = 0.075$ mm, this is described by the following solutions of Eqs. (6): $\mu_0{}^1M = 0.12$ T and $\mu_0{}^2M = 0.78$ T. In our measurements, the virgin sample was initially magnetized by a dc magnetic field to bring the magnetic system to equilibrium.

Solving Eqs. (2) for R_1 and ${}^pS_{10}$ enables one to find the axial stress ${}^pT_1$ from Eqs. (1). Using the open-circuit condition, the expression for the MEVC can be obtained in the following form:

$$\alpha_{E31} = \frac{E_3}{H_1} = -\int_{-{}^pt/2}^{{}^pt/2} \frac{{}^pd_{31}{}^pT_1}{{}^pt H_1 {}^p\varepsilon_{33}} dz, \tag{7}$$

where E_3 and H_1 are the average electric field induced across the piezoelectric layer and applied ac magnetic field, respectively. Substituting the obtained value of stress into Eq. (7) yields

$$\alpha_{E31} = -\frac{{}^pd_{31}{}^pY\mu_0({}^1M_3{}^{m1}t + {}^2M_3{}^{m2}t)tb}{\left[{}^pK_{31}^2(D^{pYpt}/_{\bar{Y}t} + b^2t^2{}^pt{}^pY) + D\left(1 - {}^pK_{31}^2\right)\right]{}^p\varepsilon_{33}}, \tag{8}$$

where the design factors are defined as follows:

$$b = \frac{{}^{m1}th_2{}^{m1}Y + (h_1 + h_2)^{m2}t^{m2}Y}{\bar{Y}t^2},$$

$$\bar{Y} = \frac{{}^{m1}t^{m1}Y + {}^{m2}t^{m2}Y + {}^pt{}^pY}{t},$$

$$D = \left[{}^{m2}Y^{m2}t(h_1 + h_2)^2 + {}^{m1}Y^{m1}th_2^2\right]\frac{{}^pt{}^pY}{t\bar{Y}} + \frac{{}^{m1}t^{m2}th_1^{2m1}Y^{m2}Y}{t\bar{Y}} + \frac{{}^pY{}^pt^3}{12\left(1 - {}^pK_{31}^2\right)} + \frac{{}^{m1}Y^{m1}t^3}{12} + \frac{{}^{m2}Y^{m2}t^3}{12}.$$

Here t is the total thickness of the sample, ${}^pK_{31}$ is the piezoelectric coupling coefficient, and Y is the Young's modulus.

Equation (8) reveals the MEVC at zero magnetostrictive coupling to be substantially determined by the piezoelectric coefficient and built-in magnetization due to using the magnetically graded components. The conclusion is that, for achieving a strong ME coupling, the magnetic layers should possess the different saturation magnetizations, $M_1s < M_2s$ and M_1s should be as large as possible.

B. Magnetoelectric effect at bending resonance

The ME coupling in the composites is known to be mediated by the mechanical stress that enables us to obtain orders-of-magnitude-stronger coupling when the frequency of the ac field is tuned to the same frequency as the longitudinal, thickness, or bending modes of the structure. For nominal sample dimensions, bending oscillations occur at lower frequencies compared with those of the longitudinal or thickness acoustic modes,[17] which is favorable for applications. Studies reveal a much higher enhancement in the strength of ME coupling for the bending mode than for other modes. Theoretical models of ME interactions at electromagnetic resonance (EMR) in a bilayer of a ferroelectric phase with a linearly graded piezoelectric coefficient and permittivity and a ferromagnetic phase with linear grading of a piezomagnetic coefficient was developed previously.[17] Here we focus on modeling the resonance ME effects at bending modes in layered structures based on PZT and stepwise-graded magnetic alloys with a no-bias magnetic field, as in Fig. 9.

Modeling of the ME effect at a zero-bias field is based on the recently reported theory of ME interactions in graded systems.[17] In contrast to Ref. 17, here the present model is based on the assumption that piezomagnetic coupling coefficients are zero: ${}^{m1}q_{ki} = {}^{m2}q_{ki} = 0$ and stepped grading in the saturation magnetization of magnetic layers results in a built-in magnetization.

The equation of bending motion of the composite, whose thickness is assumed to be small compared with other dimensions and whose width is assumed to be small compared with length, has the form[17]

$$\nabla^2\nabla^2 w + \frac{\rho t}{D}\frac{\partial^2 w}{\partial t^2} = 0, \tag{9}$$

where $\nabla^2\nabla^2$ is a biharmonic operator, w is the deflection (displacement in the z direction), t and ρ are thickness and average density of the sample, respectively, and D is the cylindrical stiffness. For a trilayer of PZT and two magnetostrictive layers, $t = {}^pt + {}^{m1}t + {}^{m2}t, \rho = ({}^p\rho\ {}^pt + {}^{m1}\rho^{m1}t + {}^{m2}\rho^{m2}t)/t$, where ${}^pt, {}^{m1}t$, and ${}^{m2}t$ are thicknesses of the piezoelectric and two piezomagnetic layers, respectively, and ${}^p\rho, {}^{m1}\rho, {}^{m2}\rho$ are the densities of the layers.

The general solution of Eq. (9) contains four arbitrary constants that have to be found from boundary conditions at $x = 0$ and $x = L$. To obtain the lowest resonance frequency possible, a cantilever of a layered piezoelectric and ferromagnetic composite is considered. For this case, the deflection and derivative of deflection $\partial w/\partial x$ equal zero at the fixed end ($x = 0$) and the turning moment J_2 and transverse force V equal zero at the free end ($x = L$). The moment of rotation is defined as

$$J_2 = \int_A zT_1 dz_1 + \mu_0 H_1({}^1M^{m1}t + {}^2M^{m2}t), \tag{10}$$

where A is the cross-sectional area of the sample normal to the x axis. The transverse force can be expressed in terms of turning moment as follows: $V = \frac{\partial J_2}{\partial x}$. The stress component T_1, which appears in the expression for the turning moment, is found from Eqs. (1), taking into account that strain components of all layers are related to the deflection of structure: $S_1 = -z\frac{\partial^2 w}{\partial x^2}$.

Taking into consideration the boundary conditions at $x = 0$ and $x = L$, solving Eq. (10) enables finding the strains and stresses. Once the stresses are determined, the MEVC can then

be found by using the open-circuit condition $\int_G {}^p D_3 dx = 0$, where G is the cross-sectional area of the sample normal to the z axis. The resultant expression for the MEVC has the form

$$\alpha_{E31} = \frac{{}^p d_{31}\,{}^p Y \mu_0 ({}^1 M_3\,{}^{m1} t + {}^2 M_3\,{}^{m2} t)(2z_0 - {}^p t)(r_1 r_4 + r_2 r_3)}{\Delta\, {}^p \varepsilon_{33}}, \tag{11}$$

where

$$\Delta = D\left[kL\left(1 + r_3^2 - r_4^2 + 2r_1 r_3\right) + 2a_1(r_1 r_4 + r_2 r_3)\right],$$

$$a_1 = \frac{1}{3D}\,{}^p K_{31}^2\,{}^p Y\,{}^p t[3z_0(z_0 - {}^p t) + {}^p t^2],$$

$r_1 = \cos(kL)$, $r_2 = \sin(kL)$, $r_3 = \cosh(kL)$, $r_4 = \sinh(kL)$,

$$k^4 = \omega^2({}^p \rho\,{}^p t + {}^{m1}\rho^{m1} t + {}^{m2}\rho^{m2} t) D^{-1},$$

$$z_0 = \frac{{}^p Y\,{}^p t^2 - {}^{m1} Y^{m1} t^2 - {}^{m2} Y^{m2} t({}^{2m1} t + {}^{m2} t)}{2({}^p Y\,{}^p t + {}^{m1} Y^{m1} t + {}^{m2} Y^{m2} t)}.$$

${}^1M$ and ${}^2M$ are the built-in magnetizations of magnetic layers arising from the stepped-graded magnetic phase. The value of this magnetization was discussed above.

One can see from Eq. (11) that for an ME interaction to occur at zero magnetostrictive coupling, the presence of internal magnetization of the magnetic phase is required. The built-in magnetization can be produced by stepped saturation magnetization. The appearance of internal magnetization can be stipulated by a compositionally graded magnetic phase as well. At EMR, the MEVC reveals an enhancement. Resonance frequencies are determined by roots of the equation $\Delta = 0$ [Δ is defined in the notation of Eq. (11)]. Coefficient a_1 that enters this equation describes the influence of piezoelectric coupling on resonance frequencies. Neglecting this influence (setting a_1 equal to zero) leads to an expression $\cos(\mathrm{kL})\cosh(\mathrm{kL}) = -1$, which coincides with that for bending vibrations of a homogeneous rod.[17]

V. APPLICATION TO PZT-NI-METGLAS

Now we carry out numerical estimates of the MEVC for samples with PZT, Ni, and Metglas. We consider ME coupling at zero bias. In this case, the sample is subjected only to ac magnetic field H_1 as in Fig. 9. The material parameters used for the estimates are listed in Table I. The energy losses are taken into account by substituting ω for complex frequency $\omega + i\omega'$ with $\omega'/\omega = 10^3$. Figure 6 shows the estimated zero-field low-frequency ME coefficient as a function number of Metglas layers L. The theory predicts dependence of the MEVC on the grading scheme due to differences in the cylindrical stiffnesses

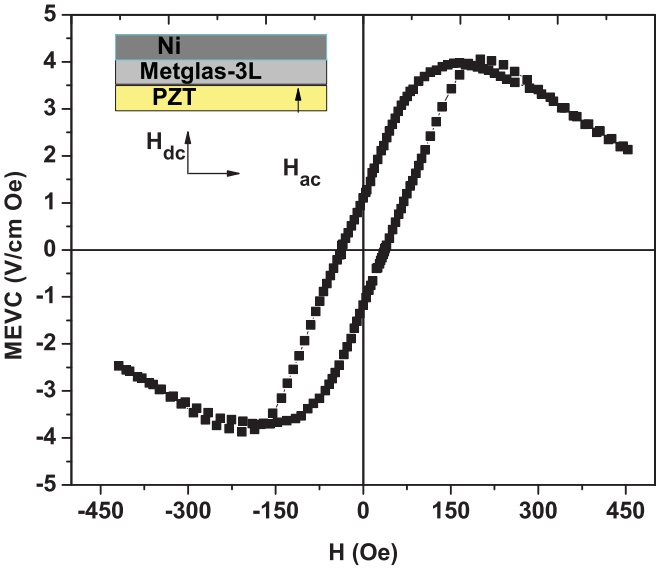

FIG. 10. (Color online) MEVC as a function of bias field H for a sample of PZT-3 L Metglas-Ni. The bias field was applied perpendicular to the sample plane, and the ac magnetic field was in-plane.

for PZT-Ni-Metglas and PZT-Metglas-Ni and an increase in the MEVC with L. The discrepancy between theory and data in Fig. 6 could be due to the fact that the theory assumes a continous magnetic medium for Metglas, whereas one has an epoxy layer between Metglas layers for $L > 1$ that gives rise to a magnetic discontinuity.

Figure 7 shows the estimated MEVC vs. frequency profile for PZT-Ni-25-μm-thick Metglas. The theoretical profile is shifted to a lower frequency compared with the data and the calculated peak MEVC is smaller than the measured value. Figure 8 shows the calculated values of the peak MEVC at bending resonance. The estimated MEVCs are higher for PZT-Ni-Metglas than for PZT-Metglas-Ni. One notices a general agreement between theory and data in Fig. 8.

It should be noted that the ground state for a magnetization-graded system has infinite solutions for the ground state. The ground states are influenced by the domain structure and the domain rearrangement brought on by an initial magnetizing field. Such samples, once magnetized to an equilibrium state, do not show any decrease in the zero-bias MEVC for a prolonged period of several months. We carried out further investigation on the nature of the zero-bias state by measuring the MEVC vs. H on a sample subjected to a transverse bias field and a longitudinal ac magnetic field. Representative results are shown in Fig. 10 for a sample of PZT-Metglas ($3L$)-Ni. For

TABLE I. Material parameters (compliance coefficient s, magnetization, permittivity ε, and density ρ) for Ni, Metglas, and PZT used for theoretical estimates. Parameters a and b are used in Eq. (5) for free-energy density.

Material	s_{11} (10^{-12} m^2/N)	$\mu_0 M$ (T)	d_31 (10^{-12} m/V)	$\varepsilon_{33}/\varepsilon_0$	ρ (g/cm^3)	a (in SI units)	b (in SI units)
PZT	15.3		175	1750	7.75		
Ni	4.9	0.616			8.9	$-1.66\cdot10^{-5}$	$0.34\cdot10^{-16}$
Metglas	10	1.56			7.18	$-2.15\cdot10^{-5}$	$0.38\cdot10^{-17}$

$|H| > 0$, the magnetoelectric coupling is due to bending of the sample under the transverse bias field and one observes an increase in the MEVC with increasing field to a maximum that is followed by a decrease in MEVC at higher fields. Upon reversal of the direction of the bias field, the MEVC begins to decrease in magnitude and is zero for $H \approx \pm 60$ Oe. For this zero-MEVC state we estimated the magnetization state of Ni and Metglas by using Eqs. (6) and obtained $\mu_0{}^1M = -0.33$ T and $\mu_0{}^2M = 0.77$ T so that the average magnetization becomes zero. Applying the dc magnetic field in the vertical direction opposite to the direction of the built-in magnetization gives rise to a decrease in the internal field in the Ni layer and an increase in the demagnetizing field in Metglas. As a result, the average magnetization approaches zero due to variations in fractions of 180° domains. Then the layers are gradually magnetized, and the average magnetization increases. So a hysteresis loop arises with the remanent magnetization equal to the built-in magnetization and a zero-bias MEVC. The sign of this zero-bias MEVC is determined by the previous magnetic state.

The data and the model discussed here are likely to encourage similar studies on functionally graded ferroics and ME interactions. Studies on monolithic heterostructures of ferroelectrics and ferromagnetics are of interest in this regard. One can, for example, grow a compositionlly graded alloy of Ni_xFe_{1-x} with x varying from 0 to 1 so that $4\pi M$ varies from 6 kG to 21 kG. Such systems are expected to show strong zero-field ME couplings that depend on only the rate of change in the magnetization.

VI. CONCLUSIONS

The observation and theory of zero-bias ME coupling have been discussed for samples of PZT and magnetization-graded ferromagnetic layers. The grading in the magnetization is achieved with the use of Ni and Metglas. A large zero-bias low-frequency ME coefficient of the order of 0.3–1.6 V/cm Oe is measured for the systems. The ME coupling is strengthened by a factor of 40 at bending modes when the samples are clamped at one end. The zero-bias ME coupling is attributed to strain-mediated coupling between the transverse magnetization due to magnetization grading at the interface of Ni-Metglas and the in-plane ac magnetic field. There is general agreement between theory and data.

ACKNOWLEDGMENTS

The research was supported by grants from the National Science Foundation, the DARPA-HUMS program, and the Army Research Office.

[1] T. Kimura, T. Goto, H. Shintani, K. Ishizaka, T. Arima, and Y. Tokura, Nature (London) **426**, 55 (2003).
[2] H. Zheng, J. Wang, S. E. Lofland, Z. Ma, L. Mohaddes-Ardabili, T. Zhao, L. Salamanca-Riba, S. R. Shinde, S. B. Ogale, F. Bai, D. Viehland, Y. Jia, D. G. Schlom, M. Wuttig, A. Roytburd, and R. Ramesh, Science **303**, 661 (2004).
[3] N. A. Spaldin and M. Fiebig, Science **309**, 391 (2005).
[4] W. Eerenstein, N. D. Mathur, and J. F. Scott, Nature (London) **442**, 759 (2006).
[5] Y.-H. Chu, L. W. Martin, M. B. Holcomb, M. Gajek, S.-J. Han, Q. He, N. Balke, C.-H. Yang, D. Lee, W. Hu, Q. Zhan, P.-L. Yang, A. Fraile-Rodríguez, A. Scholl, S. X. Wang, and R. Ramesh, Nat. Mater. **7**, 478 (2008).
[6] M. Fiebig, J. Phys. D. Appl. Phys. **38**, R123 (2005).
[7] C.-W. Nan, M. I. Bichurin, S. Dong, D. Viehland, and G. Srinivasan, J. Appl. Phys. **103**, 031101 (2008).
[8] J. Zhai, Z. Xing, S. Dong, J. Li and D. Viehland, J. Am. Ceram. Soc. **91**, 351 (2008).
[9] S. Priya, R. Islam, S. Dong, and D. Viehland, J. Elec. Ceramics **19**, 149 (2007)
[10] G. Srinivasan, Annu. Rev. Mater. Res. **40**, 153 (2010).
[11] R. A A. Islam, Y. Ni, A. G. Khachaturyan, and S. Priya, J. Appl. Phys. **104**, 044103 (2008).
[12] M. Liu, X. Li, J. Lou, S. Zheng, K. Dui and N. X. Sun, J. Appl. Phys. **102**, 083911 (2007).
[13] G. Akcay, S. Zhong, S. B. Allimi, S. P. Alpay, and J. V. Mantese, Appl. Phys. Lett. **91**, 012904 (2007).
[14] M. W. Cole, E. Ngo, S. Hirsch, J. D. Demaree, S. Zhong, and S. P. Alpay, J. Appl. Phys. **102**, 034104 (2007).
[15] M. W. Cole, E. Ngo, S. Hirsch, M. B. Okatan, and S. P. Alpay, Appl. Phys. Lett. **92**, 072906 (2008).
[16] V. M. Petrov, G. Srinivasan, and T. A. Galkina, J. Appl. Phys. **104**, 113910 (2008).
[17] V. M. Petrov and G. Srinivasan, Phys. Rev. B **78**, 184421 (2008).
[18] S. K. Mandal, G. Sreenivasulu, V. M. Petrov, and G. Srinivasan, Appl. Phys. Lett. **96**, 192502 (2010).
[19] Z.-G. Ban, S. P. Alpay, and J. V. Mantese, Phys. Rev. B **67**, 184104 (2003).
[20] A. L. Roytburd and J. Slutsker, Appl. Phys. Lett. **89**, 042907 (2006).
[21] A. L. Roytburd, S. Zhong, and S. P. Alpay, Appl. Phys. Lett. **87**, 092902 (2005).
[22] J. V. Mantese, A. L. Micheli, N. W. Schubring, R. W. Hayes, G. Srinivasan, and S. P. Alpay, Appl. Phys. Lett. **87**, 082503 (2005).
[23] C. Sudakar, R. Naik, G. Lawes, J. V. Mantese, A. L. Micheli, G. Srinivasan, and S. P. Alpay, Appl. Phys. Lett. **90**, 062502 (2007).
[24] S. Yang, C. Park, K. Cho, and S. Priya, J. Appl. Phys. **108**, 093706 (2010).
[25] V. M. Petrov, G. Srinivasan, M. I. Bichurin, and T. A. Galkina, J. Appl. Phys. **105** 063911 (2009).
[26] Z. Xing, S. Dong, Junyi Zhai, Li Yan, J. Li, and D. Viehland, Appl. Phys. Lett. **89**, 112911 (2006).
[27] J. Zhai, Z. Xing, S. Dong, J. Li, and D. Viehland, Appl. Phys. Lett. **93**, 072906 (2008).
[28] D.V. Chashin, Y. K. Fetisov, K. E. Kamentsev, and G. Srinivasan, Appl. Phys. Lett. **92**, 102511 (2008).